THE JOURNAL OF PHYSICAL CHEMISTRY Letters

Letter

pubs.acs.org/JPCL

Electroosmosis through α-Hemolysin That Depends on Alkali Cation Type

Fabien Piguet,[†] Francoise Discala,[†] Marie-France Breton,[†] Juan Pelta,[‡] Laurent Bacri,[‡] and Abdelghani Oukhaled*,[†]

[†]LAMBE UMR 8587 CNRS, Cergy University, 33 Boulevard du Port, 95000 Cergy-Pontoise, France

[‡]LAMBE UMR 8587 CNRS, Évry University, Boulevard François Mitterrand, 91000 Évry, France

Supporting Information

ABSTRACT: We demonstrate experimentally the existence of an electroosmotic flow (EOF) through the wild-type nanopore of α-hemolysin in a large range of applied voltages and salt concentrations for two different salts, LiCl and KCl. EOF controls the entry frequency and residence time of small neutral molecules (β-cyclodextrins, βCD) in the nanopore. The strength of EOF depends on the applied voltage, on the salt concentration, and, interestingly, on the nature of the cations in solution. In particular, EOF is stronger in the presence of LiCl than KCl. We interpret our results with a simple theoretical model that takes into account the pore selectivity and the solvation of ions. A stronger EOF in the presence of LiCl is found to originate essentially in a stronger anionic selectivity of the pore. Our work provides a new and easy way to control EOF in protein nanopores, without resorting to chemical modifications of the pore.

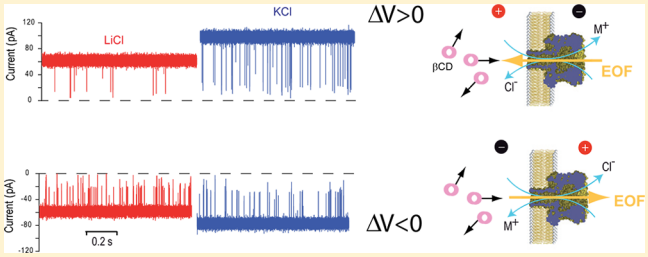

SECTION: Biophysical Chemistry and Biomolecules

Electroosmotic flow (EOF) is the movement of fluid through a capillary by the action of an electric field.[1] Today, EOF is involved in nanotechnology and fundamental biological or physical problems at the single-molecule level, such as the separation of DNA samples or chromosome isolation. EOF is also a timely subject in the nanopore translocation area; it provides a universal way to control the transport of macromolecules through a nanopore without engineering specific molecule/pore interaction. Potential applications may exist in the fast sequencing of DNA or RNA.[2,3] EOF may also be used to enhance the capture of analytes by a nanopore, thus reducing the minimal analyte concentration necessary to detect it at a pratical rate, which is of particular interest when considering expensive analytes.

Experimentally, EOF can be controlled by the electrical field, the buffer composition, the thickness of the double layer, the control of surface charges of the pore, and the viscosity of the solution.[4−11] Both protein and solid-state nanopores are under investigation to probe the effect of EOF on the transport of small molecules, synthetic macromolecules, DNA, proteins, and peptides.[4−7,12−22] In the case of the transport of charged molecules through charged nanopores, there is a combined action of diffusion, electrophoresis, and electroosmosis.[6] The quantification of the different contributions is crucial for understanding transport phenomena. In solid-state nanopores of high surface charge, it was shown recently that EOF may strongly slow down the transport of proteins or even reverse their apparent electrophoretic mobility.[6] Therefore, EOF is an important parameter to take into account in solid-state nanopore translocation. In biological nanopores, EOF is often neglected, the most popular argument being the low net charge of biological pores. Because of this idea, only few experimental studies have been devoted to electroosmosis through biological pores.[12,13,16,23,24] On the one hand, it has been demonstrated that EOF does not assist macromolecular translocations through a wild-type α-hemolysin nanopore.[13−15,25] On the other hand, Bayley and co-workers demonstrated by site-directed mutagenesis that EOF through mutant α-hemolysin nanopores may drive small neutral molecules (β-cyclodextrins, βCD) into the pore.[12] Controlling the entry and residence of βCD in the pore is of particular interest because, under appropriate conditions, βCD can act as a molecular adapter to improve nanopore detection and could be a good candidate for single-base DNA sequencing[26−28] and single-molecule mass spectrometry.[14,29−31] Nevertheless, it turns out that chemical modifications of the pore by mutagenesis are difficult to perform and require large resources.

In this Letter, we propose direct experimental evidence of EOF through the wild-type α-hemolysin nanopore without resorting to chemical modifications. We observe a voltage dependency of the entry frequency and residence time of neutral βCD in the α-hemolysin nanopore, which is interpreted as the effect of EOF through the pore. The effect of EOF is

Received: November 6, 2014
Accepted: December 1, 2014
Published: December 1, 2014

   dx.doi.org/10.1021/jz502360c | J. Phys. Chem. Lett. 2014, 5, 4362−4367

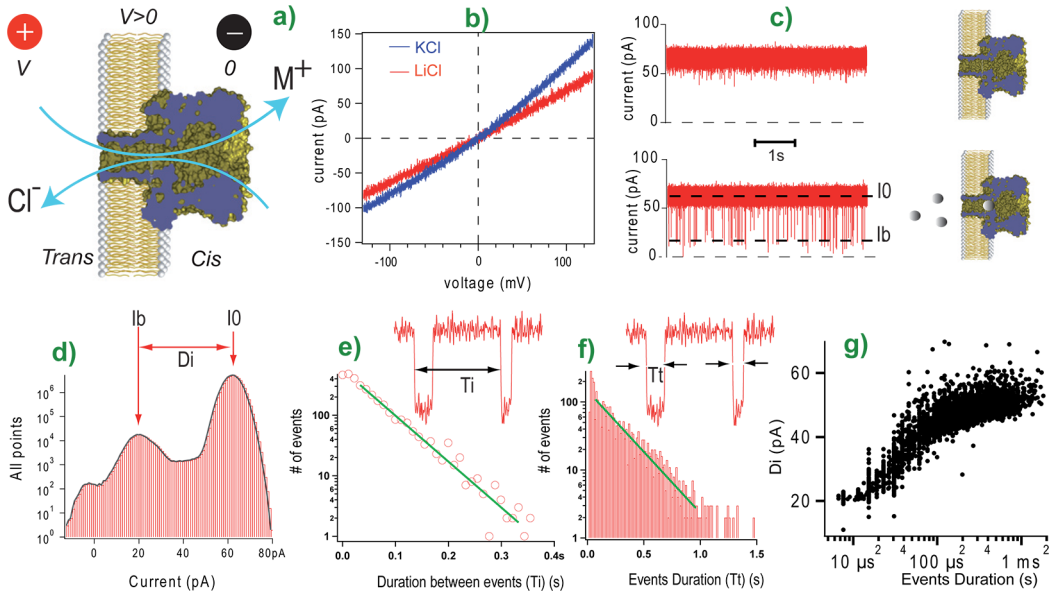

Figure 1. Experimental setup and data analysis: (a) Principle of the electrical detection method showing the ions flowing through a single α-hemolysin nanopore inserted in a lipid bilayer membrane according to the polarity sign. (b) $I-V$ curves in the presence of 1 M KCl (blue curve) or 1 M LiCl (red curve). (c) Typical current traces at 100 mV applied voltage, 1 M LiCL, in the absence (top) and presence (down) of neutral molecules (βCD). (d) Current histogram of the current trace shown in (c) (down). The interevent time T_i (e) and residence time T_t distributions (f) are shown on a log−linear plot calculated from the current trace shown in (c). The characteristic interevent time (inverse of the event frequency) and residence time are estimated from a single-exponential fit of the corresponding distributions (green solid lines). (g) Corresponding scatter plot: blockade current variation (Di) as a function of its durations.

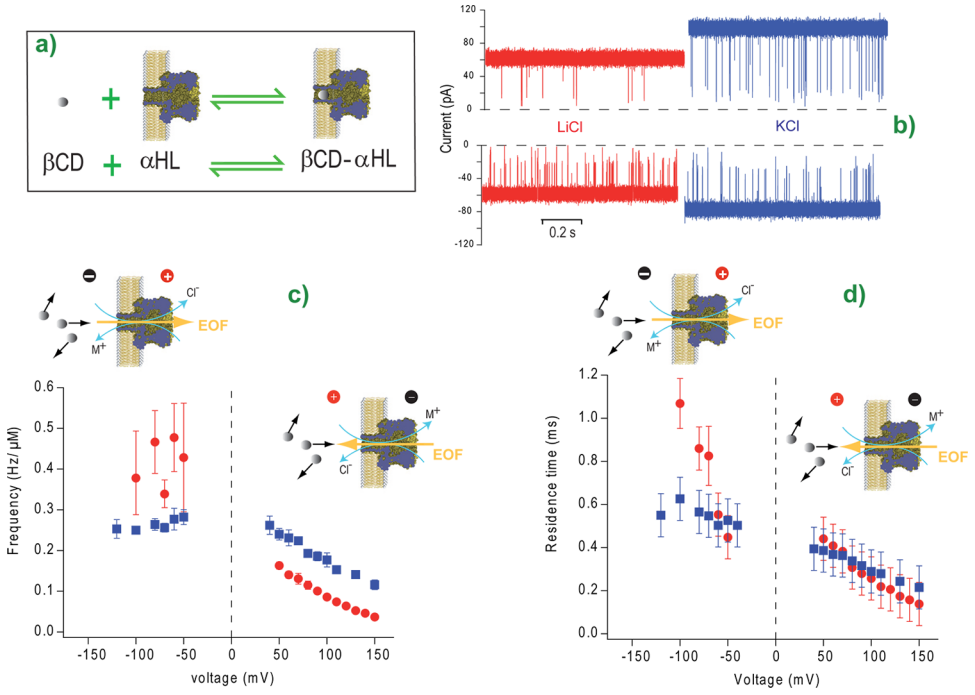

Figure 2. Experimental evidence of EOF through the α-hemolysin channel: (a) Cartoon showing the association−dissociation reaction between βCD and α-hemolysin. (b) Current traces recorded at positive voltage +100 mV (top) and negative voltage −100 mV (down) in the presence of βCD on the trans side (traces with a low current level are performed in 1 M LiCl (red), and those of a high current level are performed at 1 M KCl (blue)). Plot of the event frequency (c) or residence time (d) of βCD in the presence of 1 M LiCl (red colored circles) or 1 M KCl buffers (blue colored square) as a function of applied voltage.

investigated in a large range of applied voltages and salt concentrations for two different salts, LiCl and KCl. The nature of ions in solution has been shown to be an important parameter in the context of nanopore experiments.[15,32,33] Here, we observe that the magnitude of EOF is more significant in the presence of LiCl than KCl because of the difference of pore selectivity and solvation of ions between the two salts. Interestingly, in LiCl at physiological pH, a potentially significant EOF in the α-hemolysin is observed. In future experiments, EOF could be used to unfold small peptides, as

dx.doi.org/10.1021/jz502360c | J. Phys. Chem. Lett. 2014, 5, 4362−4367

demonstrated recently at a 2 M salt concentration and pH 3 very far from physiological conditions.[16]

The entry and residence of βCD molecules (Mw = 1135 g/mol) into the α-hemolysin nanopore are detected by using electrophysiology experiments. A lipid bilayer is prepared using a classical method[34] and separates two compartments filled by a salt buffer. The α-hemolysin nanopore is inserted into this membrane.[35] Two Ag/AgCl electrodes allow the control of the applied voltage and the measure of the ionic current. The βCD molecules are introduced on the trans side of the membrane, and the cis compartment corresponds to the one of the reference electrode (Figure 1a). In all experiments, the βCD concentration is 200 μM. We explore a large range of applied positive and negative voltages of magnitude between 30 and 150 mV using a series of buffer solutions of M^+Cl^- (with M^+ = K^+, Li^+), 0.6, 1, 2, 3, and 4 M and 5 mM HEPES, pH = 7.4. Single-channel ionic currents are recorded by an Axopatch 200B patch-clamp amplifier (Axon Instruments) in the whole-cell mode with a CV-203BU headstage. Data are acquired at 250 kHz with the DigiData 1440A digitizer coupled to the Clampex software (Axon instruments). The data are filtered using an eight-pole Bessel filter at a cutoff frequency of 10 kHz.

As our data treatment is based on a statistical analysis,[36] we detect at least 2000 events using a two-thresholds method; a first threshold th_1 is defined by the relation $th_1 = I_0 - 3\sigma$, where I_0 is the average baseline current (Figure 1d) and σ is the standard deviation of the open channel. In the histogram of the electric current (Figure 1d), one observes two populations separated by a well-defined gap. The largest population (centered at I_0) is associated with the fluctuating baseline current. The second one (centered at I_b) is associated with the blockades caused by the βCD molecules (Figure 1c). As both peaks are well discriminated, the second discrimination threshold th_2 is determined by the average between I_0 and $I_b$$th_2 = (I_0 + I_b)/2$, where I_b is the mean blockade current caused by βCD molecules (Figure 1c,d). The residence time of βCD molecules, the frequency, and the amplitude of the blockage are estimated statistically (Figure 1e−g). In most cases, each value was averaged over three different single-nanopore experiments, and the errors bars are mean standard deviations over these experiments.

It has been shown previously that the βCD molecules can enter the pore from the stem side and bind near the constriction separating the stem and vestibule parts of the pore.[26,37] The constriction is narrow enough that the βCD cannot cross it. After unbinding, the βCD escapes from the pore on the same side (stem side). The association−dissociation reaction between a βCD and α-hemolysin is shown in Figure 2a.

In Figure 2b, we show the current trace in the presence of βCD at positive (+100 mV) and negative (−100 mV) voltages by varying the salt nature. In what follows, we study in details the variation of the entry frequency and the residence time according to the applied voltage in 1 M LiCl and KCl buffer solutions (Figure 2c and d).

In 1 M LiCl, the entry frequency of βCD is always smaller for a positive applied voltage than that for a negative voltage of the same magnitude (Figure 2c). Furthermore, the residence time is always shorter for a positive voltage than that for a negative one (Figure 2d). As βCD are neutral molecules, this voltage dependency is interpreted as the effect of an EOF through the pore, in the direction of the anion current. In order to enter the pore, βCD molecules first diffuse from the trans chamber to a region near the pore entrance. Then, they begin to feel the effect of the EOF.[12,38] For a positive voltage, the EOF is directed from the cis (vestibule) to the trans (stem) side of the pore and repels the entry of βCD in the pore (see insets in Figure 2c and d). If a βCD achieves entering the pore, the cis-to-trans EOF causes the rapid ejection of βCD from the pore back to the trans chamber. For a negative voltage, the EOF is reversed. In this case, the EOF helps the entry of βCD in the pore. Once a βCD molecule is in the pore, the trans-to-cis EOF maintains βCD lodged in the stem against the pore constriction.

The voltage dependency of the entry frequency and residence time for a given voltage sign is consistent with the EOF interpretation; when the positive voltage increases, both the entry frequency and the residence time of βCD decrease because the resisting EOF increases; inversely, when the negative voltage increases in magnitude, the residence time increases because the helping EOF increases. In the negative voltage range, the entry frequency is more difficult to determine due to a greater pore instability and a worse signal/noise ratio. We observe no clear variation of the entry frequency with negative voltage. Our interpretation is that in that case, the entry frequency is determined by the diffusion time of the βCD from the bulk to the pore entrance. Once a βCD molecule is close to the pore entrance, it is quickly pulled inside of the pore, regardless of the negative voltage value.

For 1 M KCl, the entry frequency and residence time exhibit the same qualitative behavior as a function of voltage as that in LiCl (Figure 2c,d). An EOF through α-hemolysin also exists in the KCl solution. The EOF in KCl has the same qualitative voltage dependency as that in LiCl. Nevertheless, the variations of entry frequency and residence time when the voltage is reversed are smaller for KCl than those for LiCl. For positive voltages, where EOF resists the association of βCD with α-hemolysin, the entry frequencies and residence times are greater for KCl than those for LiCl. However, for negative voltages, where EOF helps the association of βCD with α-hemolysin, the entry frequencies and residence times are smaller for KCl than those for LiCl.

We propose a simple theoretical model to quantify the EOF effects through the α-hemolysin pore in our experimental conditions. Two factors contribute to the EOF, (i) the selectivity of the pore, which compares the ionic current of cations and anions through the pore,[39] and (ii) the number of solvent molecules transported by the cations and anions, respectively.[15,33]

The selectivity is quantified by evaluating the permeability ratio P_+/P_-, where the permeability P_i measures how easily ions i cross the pore (P_+ is the permeability of cations, and P_- is that of anions). If the permeability ratio is less than unity, the pore is anion-selective; otherwise, the pore is cation-selective. The Goldman−Hodgkin−Katz (GHK) equation is generally used to evaluate the permeability ratio[39]

$$\frac{P_+}{P_-} = \frac{a(X^-)_{cis} - \exp\left(-\frac{eV_r}{k_BT}\right)a(X^-)_{trans}}{\exp\left(-\frac{eV_r}{k_BT}\right)a(M^+)_{cis} - a(M^+)_{trans}} \quad (1)$$

where V_r is the reversal voltage, which sets the ionic current passing through the pore to zero; $a(X^-)$ and $a(M^+)$ are respectively the activities of anions and cations; e, k_B, and T are respectively the elementary charge, the Boltzmann constant, and the temperature.

dx.doi.org/10.1021/jz502360c | J. Phys. Chem. Lett. 2014, 5, 4362−4367

In order to measure the reversal voltage V_r for the nanopore of α-hemolysin in the presence of LiCl, we introduce different salt concentrations in cis and trans chambers, 1 M on the cis side and 0.2 M on the trans side. Agarose salt bridges containing 3 M KCl are used between electrodes and buffer solution to ensure the stability of the electrodes. In this case, we have to consider the existence of a liquid junction potential (LJP) on the interface between the salt bridge and the buffer solution, in both the cis and trans compartments.[40] The V_r measured was corrected for the LJPs using the Junction Potential Calculator, which used the Henderson equation,[40] supplied by the CLAMPEX 10.2 program. At T = 25 °C, we obtain V_r = −26 mV and thus a permeability ratio P_+/P_-(LiCl) = 0.18. This value is in agreement with previous experimental results[41] performed in slightly lower pH conditions (pH between 6 and 7 versus 7.4 here). We test the validity of our result by using the same protocol to measure the permeability ratio in the presence of KCl. We obtain P_+/P_-(KCl) = 0.71, in agreement with previous experimental results.[42] Thus, for both LiCl and KCl, the anions cross the nanopore of α-hemolysin more easily than the cations, but the selectivity to anions is greater for LiCl. It is likely that the difference of pore selectivity with cation type comes from different cation/pore interactions. Li^+ ions seem to bind more strongly to the negative charges of the pore than K^+ ions.[43,44] We note that considering the activities of the ions in solution instead of their concentration[40] does not change the permeability ratios by more than 0.02.

From the permeability ratio, one can estimate the number of water molecules flowing through the pore from the cis side to the trans side per unit time, J_w[39]

$$J_w = N_w \frac{I}{e}\left(\frac{1 - P_+/P_-}{1 + P_+/P_-}\right) \tag{2}$$

where N_w is the number of water molecules transported by an ion, assuming in a first approximation that this number is the same for a cation and for an anion; I is the ionic current flowing through the pore at a given voltage; e is the elementary charge. At 25 °C and under an applied voltage of +100 mV, typical values of the ionic current through α-hemolysin are I = 70 pA for 1 M LiCl and I = 100 pA for 1 M KCl (Figure 1b). Taking N_w = 10,[39,45] we estimate J_w(LiCl) = 3.0 × 10^9 water molecules per second and J_w(KCl) = 1.1 × 10^9 water molecules per second. The water molecule flow is stronger for LiCl than that for KCl, in agreement with our experimental observation. Note that while considering an equal number of water molecules transported by a cation and by an anion is a valid approximation for KCl, this is less the case for LiCl where Li^+ tends to be more hydrated than Cl^-.[46] As Li^+ transports more water molecules than Cl^-, this would reduce the value of J_w(LiCl) calculated above, which has the same direction as the anion current. Nevertheless, from our experimental results, we observe that the difference of hydration between Li^+ and Cl^- does not compensate for the strong anionic selectivity of the pore in the presence of these ions; the EOF for LiCl is in the direction of the anion current and is greater for LiCl than that for KCl.

The estimation of the water flow J_w leads to the calculation of the electroosmotic velocity v_{EOF}, which reads

$$v_{EOF} = \frac{J_w}{\pi r_{pore}^2 C_w} = \frac{J_w M_w}{\pi r_{pore}^2 \rho_w N_A} \tag{3}$$

where we consider the stem portion of α-hemolysin as a cylinder of radius r_{pore} containing C_w water molecules per unit volume; C_w is expressed in terms of the density of water ρ_w, the molar mass of water M_w, and Avogadro's number N_A. Taking r_{pore} = 1 nm, ρ_w = 10^3 kg/m^3 for liquid water, and M_w = 18.10^{-3} kg/mol, we obtain v_{EOF}(LiCl) = 2.9 cm/s and v_{EOF}(KCl) = 1.1 cm/s.

We compare these values to the mean transport velocity $v_{\beta CD}$ of a βCD molecule in the nanopore of α-hemolysin. If we consider that the residence of a βCD molecule in the pore corresponds to traveling from the stem extremity to the pore constrictions and then moving back to the stem extremity before escaping from the pore, we get

$$v_{\beta CD} \cong \frac{2l_{pore}}{\tau_{res}} \tag{4}$$

where l_{pore} = 5 nm is the length of the stem and τ_{res} is the residence time of the βCD molecule in the pore. At +100 mV and 1 M salt concentration, we measured τ_{res}(LiCl) = 0.26 ms and τ_{res}(KCl) = 0.29 ms (see Figure 2d). Hence $v_{\beta CD}$(LiCl) = 3.9 × 10^{-3} cm/s and $v_{\beta CD}$(KCl) = 3.5 × 10^{-3} cm/s. These values are 3 orders of magnitude smaller than the values of EOF velocities estimated from eq 3 in the same conditions. While EOF assists only one-half of the βCD transport in the pore and thus a βCD has to progress against EOF during the other half, it is likely that the binding of βCD near the pore constriction represents a large contribution to the residence time,[12,26,37,47] explaining the discrepancy that we obtain.

We also investigate experimentally the effect of salt concentration (Figure 3). We measure the entry frequency

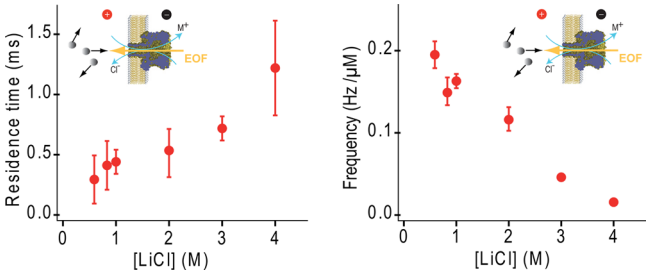

Figure 3. Effect of LiCl concentration on the residence time and event frequency. Residence time (left) and event frequency (right) as a function of LiCl salt concentration. Experiments were performed at a constant applied voltage of +50 mV.

and residence time at +50 mV for different LiCl concentrations, ranging from 0.6 to 4 M. The residence time increases when the LiCl concentration increases (Figure 3 left). When the salt concentration increases, the charges of the pore walls are more screened. This reduces the pore selectivity and hence the EOF. As for positive voltages, the EOF resists the association of βCD with the pore, and the reduction of EOF leads to larger residence times. We note that an increase of salt concentration may also affect the binding of βCD inside of the pore, which could contribute to the change of residence time. Due to the reduction of the resisting EOF, one would expect the entry frequency at fixed applied voltage (+50 mV) to increase with LiCl salt concentration. Surprisingly, the entry frequency is found to decrease as the concentration increases (Figure 3 right). We conclude that a phenomenon that varies more quickly than EOF with LiCl concentration is at the origin of the behavior of the entry frequency with LiCl concentration. The

dx.doi.org/10.1021/jz502360c | J. Phys. Chem. Lett. 2014, 5, 4362−4367

nature of this phenomenon remains an open question. One hypothesis is that the increase of salt concentration favors the self-aggregation of βCD in solution. As the diameter of the α-hemolysin pore is only slightly larger than the dimensions of one βCD molecule, such aggregates would not enter the pore. Thus, the increase in salt concentration would reduce the number of available single βCD present in the bulk chamber and which may enter the pore. Further experiments should be performed to verify this hypothesis. This point will stimulate others and us to use other technics, such as light scattering, to investigate the behavior of βCD in different salts and different ionic strengths.

We generalize our study and investigate the voltage dependence of the entry frequency and residence time for different concentrations of LiCl (1−4 M) and KCl (1−3 M) (see the Supporting Information). While most of the observations are consistent with the effect of EOF, some of them remain unexplained. For example, the behavior of the residence time with the negative voltage magnitude changes when the LiCl concentration increases from 1 to 4 M (Supporting Information Figure S1). Such a phenomenon is observed neither for the residence times at positive voltages in LiCl, nor for the residence times in KCl (Supporting Information Figure S1), nor for the entry frequencies in both LiCl and KCl (Supporting Information Figure S2). Interestingly, differences between LiCl and KCl are also observed in the dependence of the conductance of the nanopore of α-hemolysin as a function of salt concentration (Supporting Information Figure S3). While a linear behavior is observed for KCl in the concentration range (0.260−3M), the conductance for LiCl deviates from a linear behavior above 1 M and seems to saturate at higher concentrations. Further computer simulations would be necessary to elucidate if this phenomenon is related to the unexpected behavior of the entry frequency and residence time with voltage and salt concentration in LiCl.

In conclusion, an EOF is shown to control the entry frequency and residence time of small neutral molecules (βCD) in the wild-type nanopore of α-hemolysin in a wide range of LiCl and KCl salt concentrations (0.6−4 M) and applied voltages (±30 to ±150 mV). In both salts, the EOF follows the direction of the flow of anions. Depending of the voltage polarity, the EOF can either repel the βCD from the pore, decreasing both the entry frequency and residence time, or help the association of the βCD with the pore, increasing the entry frequency and residence time. The strength of the EOF depends on the voltage magnitude, on the salt concentration and, interestingly, on the nature of the cations in solution. In particular, the EOF is stronger in the presence of LiCl than KCl. This result has been interpreted by a simple theoretical model that considers the difference in pore selectivity and solvation of ions between LiCl and KCl. The larger anionic selectivity of α-hemolysin in the presence of LiCl than KCl is found to be the major contribution to the difference of EOF strength between the two salts. Although the EOF interpretation allows one to describe the larger part of our experimental results, some unexpected voltage dependencies have been observed for the entry frequency and residence time at high salt concentration. Further experiments would be necessary to understand the results obtained in these extreme salt conditions.

Our work provides an easy way to control the strength of the EOF through the widely used nanopore of α-hemolysin in standard experimental conditions, without chemical modifications of the pore. It would be interesting to probe this effect in other biological nanopores, such as aerolysine, for example. Furthermore, EOF may be used to unfold small peptides in physiological conditions, as demonstrated recently at 2 M salt concentration and pH 3 very far from physiological conditions.[16] Finally, reducing the pore diameter with a molecular adapter as a βCD molecule could be useful to enhance analyte detection, sequencing, or single-molecule spectrometry.[14,29,30,48] In this context, it would be interesting to investigate deeply if an EOF could block a βCD in the pore for sufficiently long times, without chemical modifications of the pore.

■ ASSOCIATED CONTENT

Supporting Information

Figure S1: Effect of the applied voltage on the residence time of the neutral βCD molecules in different LiCl and KCl salt concentrations. Figure S2: Effect of the applied voltage on the entry frequency of the neutral βCD molecules in different LiCl and KCl concentrations. Figure S3: α-Hemolysin conductivity for different LiCl and KCl concentrations. This material is available free of charge via the Internet at http://pubs.acs.org.

■ AUTHOR INFORMATION

Corresponding Author

*E-mail: abdelghani.oukhaled@u-cergy.fr.

Notes

The authors declare no competing financial interest.

■ ACKNOWLEDGMENTS

This work was supported by DIM-NANO-K TRANS LOCPROT No. 094251, la région Ile-de-France and the French Agence Nationale de la Recherche ANR-12-NANO-0012-03. We thank Jan Behrends (Institute of Physiology, University of Freiburg) and Loïc Auvray (Matière et Systèmes Complexes, UMR 7057 CNRS, Université Paris 7 Diderot) for stimulating and useful discussions.

■ REFERENCES

(1) Reuss, F. F. Notice sur un Nouvel Effet de l'Électricité Galvanique. *Mém. Soc. Naturalistes Moscou* **1809**, *2*, 327−337.

(2) Keyser, U. F.; Koeleman, B. N.; van Dorp, S.; Krapf, D.; Smeets, R. M. M.; Lemay, S. G.; Dekker, N. H.; Dekker, C. Direct Force Measurements on DNA in a Solid-State Nanopore. *Nat. Phys.* **2006**, *2*, 473−477.

(3) van Dorp, S.; Keyser, U. F.; Dekker, N. H.; Dekker, C.; Lemay, S. G. Origin of the Electrophoretic Force on DNA in Solid-State Nanopores. *Nat. Phys.* **2009**, *5*, 347−351.

(4) Miller, S. A.; Young, V. Y.; Martin, C. R. Electroosmotic Flow in Template-Prepared Carbon Nanotube Membranes. *J. Am. Chem. Soc.* **2001**, *123*, 12335−12342.

(5) Miller, S. A.; Martin, C. R. Redox Modulation of Electroosmotic Flow in a Carbon Nanotube Membrane. *J. Am. Chem. Soc.* **2004**, *126*, 6226−6227.

(6) Firnkes, M.; Pedone, D.; Knezevic, J.; Doblinger, M.; Rant, U. Electrically Facilitated Translocations of Proteins through Silicon Nitride Nanopores: Conjoint and Competitive Action of Diffusion, Electrophoresis, and Electroosmosis. *Nano Lett.* **2010**, *10*, 2162−2167.

(7) Yusko, E. C.; An, R.; Mayer, M. Electroosmotic Flow Can Generate Ion Current Rectification in Nano- and Micropores. *ACS Nano* **2010**, *4*, 477−487.

(8) Brechtel, R.; Hohmann, W.; Rüdiger, H.; Wätzig, H. Control of the Electroosmotic Flow by Metal-Salt-Containing Buffers. *J. Chromatogr., A* **1995**, *716*, 97−105.

(9) Kuo, T.-C.; Sloan, L. A.; Sweedler, J. V.; Bohn, P. W. Manipulating Molecular Transport through Nanoporous Membranes by Control of Electrokinetic Flow: Effect of Surface Charge Density and Debye Length. *Langmuir* **2001**, *17*, 6298−6303.
(10) Polson, N. A.; Hayes, M. A. Electroosmotic Flow Control of Fluids on a Capillary Electrophoresis Microdevice Using an Applied External Voltage. *Anal. Chem.* **2000**, *72*, 1088−1092.
(11) Wang, S.-C.; Perso, C. E.; Morris, M. D. Effects of Alkaline Hydrolysis and Dynamic Coating on the Electroosmotic Flow in Polymeric Microfabricated Channels. *Anal. Chem.* **2000**, *72*, 1704−1706.
(12) Gu, L.-Q.; Cheley, S.; Bayley, H. Electroosmotic Enhancement of the Binding of a Neutral Molecule to a Transmembrane Pore. *Proc. Natl. Acad. Sci. U.S.A.* **2003**, *100*, 15498−15503.
(13) Wong, C. T. A.; Muthukumar, M. Polymer Translocation through α-Hemolysin Pore with Tunable Polymer−Pore Electrostatic Interaction. *J. Chem. Phys.* **2010**, *133*, 045101.
(14) Reiner, J. E.; Kasianowicz, J. J.; Nablo, B. J.; Robertson, J. W. F. Theory for Polymer Analysis Using Nanopore-Based Single-Molecule Mass Spectrometry. *Proc. Natl. Acad. Sci. U.S.A.* **2010**, *107*, 12080−12085.
(15) Breton, M. F.; Discala, F.; Bacri, L.; Foster, D.; Pelta, J.; Oukhaled, A. Exploration of Neutral Versus Polyelectrolyte Behavior of Poly(ethylene glycol)s in Alkali Ion Solutions Using Single-Nanopore Recording. *J. Phys. Chem. Lett.* **2013**, *4*, 2202−2208.
(16) Mereuta, L.; Roy, M.; Asandei, A.; Lee, J. K.; Park, Y.; Andricioaei, I.; Luchian, T. Slowing Down Single-Molecule Trafficking through a Protein Nanopore Reveals Intermediates for Peptide Translocation. *Sci. Rep.* **2014**, *4*, 3885.
(17) Sun, L.; Crooks, R. M. Single Carbon Nanotube Membranes: A Well-Defined Model for Studying Mass Transport through Nanoporous Materials. *J. Am. Chem. Soc.* **2000**, *122*, 12340−12345.
(18) Vogel, R.; Anderson, W.; Eldridge, J.; Glossop, B.; Willmott, G. A Variable Pressure Method for Characterizing Nanoparticle Surface Charge Using Pore Sensors. *Anal. Chem.* **2012**, *84*, 3125−3131.
(19) German, S. R.; Luo, L.; White, H. S.; Mega, T. L. Controlling Nanoparticle Dynamics in Conical Nanopores. *J. Phys. Chem. C* **2013**, *117*, 703−711.
(20) Luo, L.; Holden, D. A.; White, H. S. Negative Differential Electrolyte Resistance in a Solid-State Nanopore Resulting from Electroosmotic Flow Bistability. *ACS Nano* **2014**, *8*, 3023−3030.
(21) Oukhaled, A.; Cressiot, B.; Bacri, L.; Pastoriza-Gallego, M.; Betton, J.-M.; Bourhis, E.; Jede, R.; Gierak, J.; Auvray, L.; Pelta, J. Dynamics of Completely Unfolded and Native Proteins through Solid-State Nanopores as a Function of Electric Driving Force. *ACS Nano* **2011**, *5*, 3628−3638.
(22) Oukhaled, A.; Bacri, L.; Pastoriza-Gallego, M.; Betton, J.-M.; Pelta, J. Sensing Proteins through Nanopores: Fundamental to Applications. *ACS Chem. Biol.* **2012**, *7*, 1935−1949.
(23) Rosenberg, P. A.; Finkelstein, A. Water Permeability of Gramicidin A-Treated Lipid Bilayer Membranes. *J. Gen. Physiol.* **1978**, *72*, 341−350.
(24) Levitt, D. G.; Elias, S. R.; Hautman, J. M. Number of Water Molecules Coupled to the Transport of Sodium, Potassium and Hydrogen Ions via Gramicidin, Nonactin or Valinomycin. *Biochim. Biophys. Acta, Biomembr.* **1978**, *512*, 436−451.
(25) Maglia, G.; Restrepo, M. R.; Mikhailova, E.; Bayley, H. Enhanced Translocation of Single DNA Molecules through α-Hemolysin Nanopores by Manipulation of Internal Charge. *Proc. Natl. Acad. Sci. U.S.A.* **2008**, *105*, 19720−19725.
(26) Gu, L.-Q.; Braha, O.; Conlan, S.; Cheley, S.; Bayley, H. Stochastic Sensing of Organic Analytes by a Pore-Forming Protein Containing a Molecular Adapter. *Nature* **1999**, *398*, 686−690.
(27) Astier, Y.; Braha, O.; Bayley, H. Toward Single Molecule DNA Sequencing: Direct Identification of Ribonucleoside and Deoxyribonucleoside 5′-Monophosphates by Using an Engineered Protein Nanopore Equipped with a Molecular Adapter. *J. Am. Chem. Soc.* **2006**, *128*, 1705−1710.
(28) Wu, H.-C.; Astier, Y.; Maglia, G.; Mikhailova, E.; Bayley, H. Protein Nanopores with Covalently Attached Molecular Adapters. *J. Am. Chem. Soc.* **2007**, *129*, 16142−16148.
(29) Robertson, J. W. F.; Rodrigues, C. G.; Stanford, V. M.; Rubinson, K. A.; Krasilnikov, O. V.; Kasianowicz, J. J. Single-Molecule Mass Spectrometry in Solution Using a Solitary Nanopore. *Proc. Natl. Acad. Sci. U.S.A.* **2007**, *104*, 8207−8211.
(30) Baaken, G.; Ankri, N.; Schuler, A.-K.; Rühe, J.; Behrends, J. C. Nanopore-Based Single-Molecule Mass Spectrometry on a Lipid Membrane Microarray. *ACS Nano* **2011**, *5*, 8080−8088.
(31) Angevine, C. E.; Chavis, A. E.; Kothalawala, N.; Dass, A.; Reiner, J. E. Enhanced Single Molecule Mass Spectrometry via Charged Metallic Clusters. *Anal. Chem.* **2014**, *86*, 11077−11085.
(32) Gurnev, P. A.; Harries, D.; Parsegian, V. A.; Bezrukov, S. M. The Dynamic Side of the Hofmeister Effect: A Single-Molecule Nanopore Study of Specific Complex Formation. *ChemPhysChem* **2009**, *10*, 1445−1449.
(33) Rodrigues, C. G.; Machado, D. C.; da Silva, A. M.; Junior, J. J.; Krasilnikov, O. V. Hofmeister Effect in Confined Spaces: Halogen Ions and Single Molecule Detection. *Biophys. J.* **2011**, *100*, 2929−2935.
(34) Mueller, P.; Rudin, D. O.; Tien, H. T.; Wescott, W. C. Methods for the Formation of Single Bimolecular Lipid Membranes in Aqueous Solution. *J. Phys. Chem.* **1963**, *67*, 534−535.
(35) Kasianowicz, J. J.; Brandin, E.; Branton, D.; Deamer, D. W. Characterization of Individual Polynucleotide Molecules Using a Membrane Channel. *Proc. Natl. Acad. Sci. U.S.A.* **1996**, *93*, 13770−13773.
(36) Merstorf, C.; Cressiot, B.; Pastoriza-Gallego, M.; Oukhaled, A.; Betton, J.-M.; Auvray, L.; Pelta, J. Wild Type, Mutant Protein Unfolding and Phase Transition Detected by Single-Nanopore Recording. *ACS Chem. Biol.* **2012**, *7*, 652−658.
(37) Gu, L.-Q.; Bayley, H. Interaction of the Noncovalent Molecular Adapter, β-Cyclodextrin, with the Staphylococcal α-Hemolysin Pore. *Biophys. J.* **2000**, *79*, 1967−1975.
(38) Muthukumar, M. Theory of Capture Rate in Polymer Translocation. *J. Chem. Phys.* **2010**, *132*, 195101.
(39) Hille, B. *Ionic Channels of Excitable Membranes*; Sinauer Associates: Sunderland, U.K., 1992.
(40) Barry, P.; Lynch, J. Liquid Junction Potentials and Small Cell Effects in Patch-Clamp Analysis. *J. Membr. Biol.* **1991**, *121*, 101−117.
(41) Chakraborty, T.; Schmid, A.; Notermans, S.; Benz, R. Aerolysin of Aeromonas sobria: Evidence for Formation of Ion-Permeable Channels and Comparison with Alpha-Toxin of Staphylococcus aureus. *Infect. Immun.* **1990**, *58*, 2127−2132.
(42) Mohammad, M. M.; Movileanu, L. Impact of Distant Charge Reversals within a Robust β-Barrel Protein Pore. *J. Phys. Chem. B* **2010**, *114*, 8750−8759.
(43) Aziz, E. F.; Ottosson, N.; Eisebitt, S.; Eberhardt, W.; Jagoda-Cwiklik, B.; Vácha, R.; Jungwirth, P.; Winter, B. Cation-Specific Interactions with Carboxylate in Amino Acid and Acetate Aqueous Solutions: X-ray Absorption and Ab Initio Calculations. *J. Phys. Chem. B* **2008**, *112*, 12567−12570.
(44) Bhattacharya, S.; Muzard, J.; Payet, L.; Mathé, J.; Bockelmann, U.; Aksimentiev, A.; Viasnoff, V. Rectification of the Current in α-Hemolysin Pore Depends on the Cation Type: The Alkali Series Probed by Molecular Dynamics Simulations and Experiments. *J. Phys. Chem. C* **2011**, *115*, 4255−4264.
(45) Aksimentiev, A.; Schulten, K. Imaging α-Hemolysin with Molecular Dynamics: Ionic Conductance, Osmotic Permeability, and the Electrostatic Potential Map. *Biophys. J.* **2005**, *88*, 3745−3761.
(46) Israelachvili, J. *Intermolecular and Surface Forces*; Academic Press: San Diego, CA, 1991.
(47) Gu, L. Q.; Cheley, S.; Bayley, H. Prolonged Residence Time of a Noncovalent Molecular Adapter, β-Cyclodextrin, within the Lumen of Mutant α-Hemolysin Pores. *J. Gen. Physiol.* **2001**, *118*, 481−94.
(48) Balijepalli, A.; Ettedgui, J.; Cornio, A. T.; Robertson, J. W. F.; Cheung, K. P.; Kasianowicz, J. J.; Vaz, C. Quantifying Short-Lived Events in Multistate Ionic Current Measurements. *ACS Nano* **2014**, *8*, 1547−1553.